


¹⁴C-AMS TECHNOLOGY AND ITS APPLICATIONS TO AN OIL FIELD TRACER EXPERIMENT

Hongtao Shen^{1,2*}  • Shulin Shi^{1,†} • Junsen Tang^{1*} • Mingli Qi¹ • Siyu Wei¹ • Kimikazu Sasa³ • Mingji Liu¹ • Li Wang¹ • Guofeng Zhang¹ • Linjie Qi¹ • Dingxiong Chen¹ • Shanhua Gong⁴ • Guofu Song⁴ • Junyan Dong⁴ • Ning Wang^{1,2} • Houbing Zhou^{1,2} • Ming He⁵ • Qingzhang Zhao⁵ • Mingjun Wei⁴ • Yun He^{1,2*}

¹Guangxi Normal University, College of Physics and Technology, Guangxi Normal University, Guilin 541004, China

²Guangxi Key Laboratory of Nuclear Physics and Technology, Guilin 541004, China

³University of Tsukuba, Tsukuba, Ibaraki 305-8577, Japan

⁴Research Institute of Production Engineering and Technology, Zhongyuan Oilfield Company, SINOPEC, Puyang 457001, China

⁵China Institute of Atomic Energy, Beijing 102413, China

ABSTRACT. Many waterflooding oil fields, injecting water into an oil-bearing reservoir for pressure maintenance, are in their middle to late stages of development. To explore the geological conditions and improve oilfield recovery of the most important well group of the Hu 136 block, located on the border areas of three provinces (Henan, Shandong, and Hebei), Zhongyuan Oilfield, Sinopec, central China, a ¹⁴C cross-well tracer monitoring technology was developed and applied in monitoring the development status and recognize the heterogeneity of oil reservoirs. The tracer response in the production well was tracked, and the water drive speed, swept volume of the injection fluid were obtained. Finally, the reservoir heterogeneity characteristics, such as the dilution coefficient, porosity, permeability, and average pore-throat radius, were fitted according to the mathematical model of the heterogeneous multi-layer inter-well theory. The ¹⁴C-AMS technique developed in this work is expected to be a potential analytical method for evaluating underground reservoir characteristics and providing crucial scientific guidance for the mid to late oil field recovery process.

KEYWORDS: AMS, ¹⁴C, oil field, tracer, water sample preparation.

INTRODUCTION

At present, the world's oil and gas industry is undergoing significant qualitative changes. In different countries and regions, these changes have their own specific features, but there is a common theme that the future oil supply will decline (Höök et al. 2009; Al-Fattah 2020). Most oil fields are now in the process of secondary or tertiary oil recovery. Therefore, a complete understanding of the properties of highly permeable aquifers, such as water drive speed, swept volume, permeability, and radius of pore passages, have become an urgent problem to be solved (Lake 1989). However, at present, chemical tracers are mainly used for oil field monitoring by Zhongyuan Oilfield, Sinopec, China. The most significant disadvantages of chemical tracers include: the large amount used, high cost, and increment of background value due to long-term use, eventually affecting the tracer effect, while the advantages of ¹⁴C tracing in cross-well experiments include: a low background, negligible radioactivity hazard, and capability for high-precision measurements, making it an ideal cross-well tracer. To overcome those aforementioned difficulties and to scientifically guide extraction in mid to late development stages, a ¹⁴C isotope tracer combined with a highly sensitive accelerator mass spectrometry was developed and applied in this oilfield inter-well monitoring study.

The physical and chemical properties of the tracer, the characteristics of the oil field reservoir, and the injected medium should be considered to ensure that the tracer can accurately track the injected fluid after being introduced to the water well and obtain a complete and accurate tracer

[†]These authors contributed equally to this work.

*Corresponding authors. Emails: shenht@gxnu.edu.cn; Tangjs@gxnu.edu.cn; hy@gxnu.edu.cn.

response curve. Thus, the tracer interpretation results should be consistent with the actual formation of the fluid dynamics. The tracers have the following screening criteria: (1) the background content of the tracer in the formation and injected water should be low, the detection method should be simple, and the sensitivity should be high; (2) the tracer is easily soluble in water and hardly in oil, and the best partition coefficient between oil and water is close to zero; (3) after the tracer is mixed with the formation water, it is not easy to cause a chemical reaction that causes the tracer to be lost, resulting in precipitation or isotope exchange; (4) the tracer can exist stably in the formation, that is, it has the characteristics of temperature resistance, acid resistance, alkali resistance, and is not easily ingested by bacteria; (5) the amount of tracer absorbed in the formation is small, to minimize the loss of the tracer due to formation adsorption.

The trace time for cross wells in the oil field can generally take several months and up to a year to be monitored. Therefore, the long-lived radionuclide, ^{14}C -labeled urea ($\text{CO}(\text{NH}_2)_2$), was chosen as a tracer to carry out the tracer experiments. Although ^{14}C is a radioactive isotope, it is a pure beta emitter with an energy of only 156 keV and a short biological half-life (meaning it can be excreted quickly), making it a safe and feasible tracer. As a water-soluble compound, urea is easily soluble in water but hardly soluble in oil. The aqueous urea solution could be hydrolyzed very slowly beyond 80°C to generate NH_3 and CO_2 (Rahimpur et al. 2004; Sahu et al. 2011), which could be dissolved in water in the form of HCO_3^- or CO_3^{2-} , and continue to be pushed forward with the flushing of a large amount of water. Therefore, ^{14}C -labeled urea could be an ideal tracer for cross-well monitoring.

MATERIALS AND METHODS

Sites and Sampling

Calculation of Tracer Dosage

The tracer dosage was calculated based on the method of the total dilution model, which assumes that after the tracer is injected into the oil field, it can be evenly distributed over the entire swept volume. According to the calculation formula for the tracer total dilution model (Zemel et al. 1995):

$$Q = V \times L \times T \quad (1)$$

where, V is the maximum swept volume, L is the background concentration, and T is the multiple of the tracer background concentration, generally taken as 100. The formula for calculating the maximum swept volume is:

$$V = 3.14R^2H\phi S_w K_c \quad (2)$$

where, R is the average radius of the well group (m), H is the average thickness of the oil layer (m), ϕ is the average porosity (%), S_w is the water saturation (%), and K_c is the well net correction coefficient, taken as 1. A blank sample from the subject oil well H136-C1 was taken, prepared, and measured using AMS to calculate L . The sample preparation results show that the carbon content in the oil-water sample is ~ 50 mg/L, and the AMS measurement result shows that the $^{14}\text{C}/^{12}\text{C}$ abundance value in the oil-water sample is below 5×10^{-14} , and the number of ^{14}C atoms was deduced to be approximately 1.25×10^8 atoms/L. Substituting the oil field parameters into formula (2), the calculated V is 1.106×10^8 L, and then the ^{14}C tracer injection atom number Q is calculated to be 1.383×10^{18}

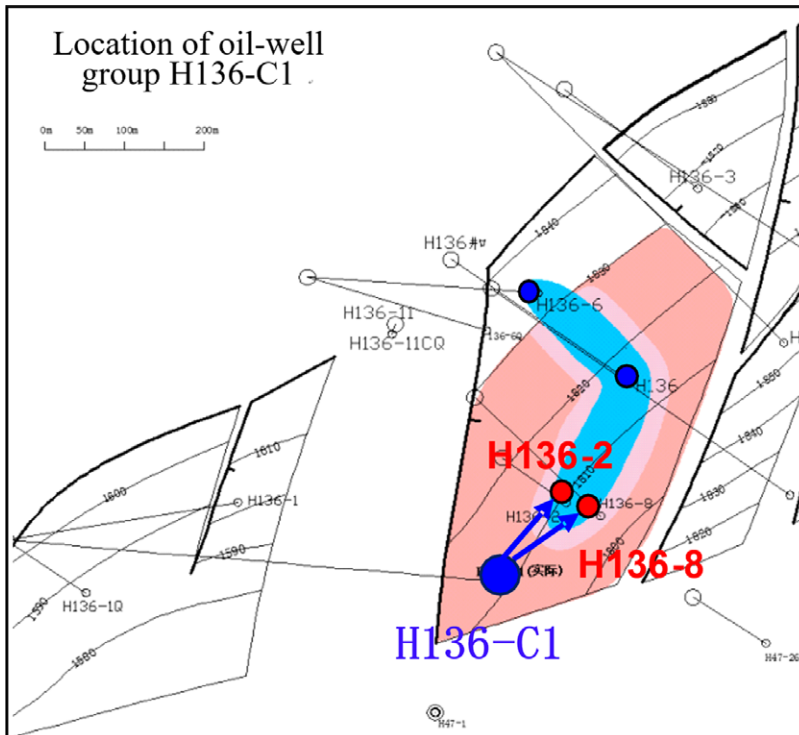


Figure 1 Location of oil-well group H136-C1, H136-2, and H136-8Fig.

using formula (1). We used a total calculated to be 3.08×10^{18} ^{14}C atoms in this tracer experiment, using 360uCi of ^{14}C in the form of commercial urea enriched to 99% in ^{14}C .

Tracer Experiment and Sampling

The target-well group of the Hu 136 block (Figure 1), including one water-well (Hu136-C1) and two oil wells (H136-2, H136-8), is located on the border areas of three provinces (Henan, Shandong, and Hebei), 200 km northeast of Zhenzhou in the Henan Province, 200 km southwest of Jinan in the Shandong Province, and 250 km southeastern from Shijiazhuang in the Hebei Province, central China. The GPS coordinates are $35^{\circ}51'58''\text{N}$, $115^{\circ}20'24''\text{E}$, and the altitude was 58 m. The area's mean annual rainfall and temperature are 565 mm and 13.3°C , respectively (Zhong et al. 2008; Gao and Tian 2009). The oil-bearing area of the well group is 0.36 km^2 , the controlled geological reserves are $42.24 \times 10^4 \text{ t}$, and the recoverable reserves are $11 \times 10^4 \text{ t}$. The target-well group is one of medium porosity and low permeability type well group. The original advancing speed of the main slug of the injected water is less than 2 m/d. The original formation pressure is about 25.4MPa, and the geothermal gradient is about $4.1^{\circ}\text{C}/100 \text{ m}$.

A pump and 10 m^3 water tank trucks were used at the tracer injection site. The ^{14}C -labeled urea capsules were first dissolved in 2 L of hot water at a temperature of 40°C on-site for 5 min and then placed in a water tank with 10 m^3 40°C hot water. After fully dissolving in hot water, the ^{14}C tracer was injected into the water well within 2 hr. The specific injection process steps were as follows: (1) inspect the wellhead to ensure tight sealing of valves and pipelines; (2) connect

the water tank truck, pump truck, and pipeline of the injection wellhead; (3) the pressure test was conducted at 30 MPa to ensure that the pressure drop was less than 0.7 MPa within 30 min and there was no leakage at all parts of the injection pipeline; (4) inject tracer with pump truck. The whole process lasted for ~2 hr; (5) the water valve was opened to resume the regular water injection. After the on-site tracer injection, sampling was started in the two oil wells on the same day. Approximately 1000 mL of oil-water samples were taken after being drained for 2–5 min to eliminate dead oil for each monitoring well. The sampling frequency was usually once per day and could be appropriately increased when a tracer was found. After all the peaks appeared, the sampling frequency was gradually reduced from 1 time/2 d to 1 time/4 d to extend the sampling time until sampling was stopped. The obtained samples were labeled with the date and well number before being sent to the AMS laboratory more than 1000 km away for preparation.

Sample Preparation

For each oil-water sample, approximately 300 mL solution was subjected to oil-water separation by decanting it into a 500 mL round-bottom flask through a 0.45 μm PTFE membrane vacuum filter. The flask bottle was then attached to a bubbler of the vacuum line for CO_2 production and purification. The sample preparation line was divided into the CO_2 bubbling circulation area (dotted line portion) and the CO_2 purification collection area. The main vacuum line in the CO_2 purification collection area was made of quartz glass, and the CO_2 bubbling circulation line was a metal pipeline. Before CO_2 extraction, the bubbling circulation line was first flushed with high-purity nitrogen for a minimum of 5 min (typical pressure value of 1050 mbar) to remove any air CO_2 presents in the metal pipeline and the glass reaction line. The circulation line was then closed, vacuumed to a pressure of approximately 800 mbar, and 4 mL of 85% H_3PO_4 (in the funnel of the upper part of the bubbler) was introduced into the water solution. A part of the phosphoric acid should be left in the glass funnel to prevent outside air from entering the cycle. At this time, phosphoric acid entered the round-bottom flask and reacted with urea or carbonate in the water to form CO_2 . When the two cold traps at -90°C and one nitrogen trap at -196°C were in place, and all the valves in the circulation loop were open, a recirculating diaphragm pump was turned on, forcing the carrier gas through the heated flask at 60°C , and producing a stream of fine bubbles throughout the solution. The CO_2 gas first passes through two cold traps at -90°C to thoroughly remove the water vapor and then enters the cold trap at -196°C , where it is frozen. After 10 min of circulation, the pump was shut off and the N_2 carrier gas was slowly pumped away. The liquid nitrogen baths on the loop traps were removed, and the CO_2 was collected in a calibrated volume, where the gas pressure was recorded and used to calculate the concentration of CO_2 in each sample. The typical yields for water samples are ca. 1 mmol of CO_2 , and only ca. 0.07 mmol of CO_2 (containing 1 mg C) was transferred to a reduction tube for graphite target preparation. While the sample was being quantified, a vacuum line was prepared for the next sample. The average analysis time was approximately 20 min. The reduction process of graphite was carried out in the closed system of the reduction reaction tube, in which 2.5 mg of iron powder and 35 mg of zinc powder were put in advance into a small tube (inner diameter 4 mm) and the reducing tube (inner diameter 8 mm), respectively, and was pretreated at 400°C for 2 hr. The reduction tube with purified CO_2 was then placed in a muffle furnace at 600°C for 8 hr to undergo a full reduction reaction. Finally, the graphite adhered to the iron powder in the reduction tube and was pressed into the AMS cathode for AMS



Figure 2 A single-stage 200 kV AMS system at GXNU.

measurements. The $^{14}\text{C}/^{12}\text{C}$ ratio of the process blank (2.5 mg IAEA-C₁ dissolved in 50 mL deionized water) prepared with this water sample preparation system was below 2×10^{-14} .

^{14}C -AMS Measurement at GXNU

The 0.2 MV AMS facility at the Guangxi Normal University (GXNU), a homemade system shown in Figure 2, was used for routine analyses of ^{14}C (He et al. 2019; Shen et al. 2019). The details of the ^{14}C -AMS measurements were as follows: first, the graphite samples with the iron powder were pressed into an Al sample holder in a 40-sample target wheel. The C- anions were extracted, selected by an injection magnet, and injected into a 0.2MV single-stage accelerator. The vacuum chamber of the injection magnet is insulated and connected to acceleration gaps on the entrance and exit sides, which allowed for a fast sequential injection of different isotopes into the accelerator by applying high-voltage pulses to the magnet chamber. In this way, the energies of ^{12}C , ^{13}C , and ^{14}C ions with different masses were adjusted, resulting in the same magnetic rigidity inside the magnet. A terminal voltage of 0.2 MV was used for acceleration, and ^{14}C ions with 1+ charge state were selected by analyzing the magnet after He gas stripping and passing through a 90° electrostatic analyzer. They were then recorded using a silicon detector. At present, the background level was $^{14}\text{C}/^{12}\text{C} \sim 3 \times 10_3^{-15}$ with a commercial graphite sample from Alfa Aesar Co.

The simulation transport procedure for C was as follows: first, a commercial graphite sample was used, and ^{13}C - ions were extracted from the ion source to simulate the ^{14}C beam transport of a standard sample. The voltages applied to the magnet chamber and the terminal were set to ensure that the $^{13}\text{C}^+$ ions would have the same energy as the $^{14}\text{C}^+$ ions. The electric and magnetic parameters of the ion optics system were tuned to determine the optimum state of the beam transport. Next, all magnets were scaled up from mass 13 to mass 14. Then, the

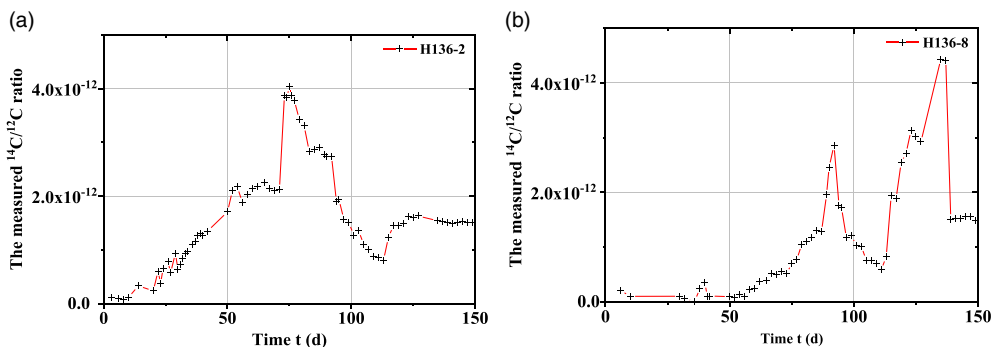


Figure 3 The tracer concentration curve for well H136-2 (a) and H136-8 (b). The dot represents the AMS measurement data.

standard sample was used, and $^{14}\text{C}^-$ ions were extracted from the ion source and passed through the injection magnet, accelerator, analyzing magnet, electrostatic analyzer, and finally recorded by a silicon detector.

The transmission efficiency of ^{14}C was approximately 50% for charge state 1^+ . The relatively high efficiency of the ^{14}C measurement enabled the measurement of more than 60 samples per day. The $^{14}\text{C}/^{12}\text{C}$ values were determined by normalizing the measured values against the values of a series of standard samples (NIST-SRM4990C, IAEA-C1, and IAEA-C8). Five 5-min runs were performed for each sample. The abundance values were based on the averages, and the uncertainties were based on the relative standard deviations of the five runs and counting uncertainty.

RESULTS AND DISCUSSION

Tracer Production Curve

After the tracer injection, the tracer concentrations of the production wells H136-2 and H136-8 were measured by AMS from October 30, 2020, to March 27, 2021. The monitoring period was 149 days and 298 samples, half of which were measured. Each sample was measured five times. The relative standard deviation (RSD) of the $^{14}\text{C}/^{12}\text{C}$ values for each sample ranged from 0.5 to 1% (0.8%, median). The $^{14}\text{C}/^{12}\text{C}$ ratios results obtained by AMS were then converted to the unit in the form of radioactivity concentration Bq/kg C. The tracer concentration production curves for both production wells are shown in Figure 3. The output curve clearly shows that the tracer was seen on the 20th day in the H136-2 well, and the concentration peak was on the 65th, 77th, and 127th day. For the H136-8 well, the tracer was seen on the 54th day, and the peak was on the 92nd and 135th days. The AMS measurement data show that the background $^{14}\text{C}/^{12}\text{C}$ ratio of the oil-water samples was about 5×10^{-14} , the peak $^{14}\text{C}/^{12}\text{C}$ ratio was about 4×10^{-12} (800 Bq/kg C), which is consistent with our previous calculation, and it was experimentally verified that the ^{14}C -labeled urea is an ideal tracer for cross-well monitoring.

Mathematical Model

According to the modified mathematical model of the heterogeneous multi-layer inter-well tracer concentration curve established by Lake (1989), as shown in Eq. (3).

$$C_D = \frac{a}{2} \operatorname{erfc} \left(\frac{x_D - \frac{r_n}{\bar{r}} t_D}{2 \sqrt{\frac{r_n}{\bar{r}} \alpha_D t_D}} \right) - \frac{a}{2} \operatorname{erfc} \left(\frac{x_D - \frac{r_n}{\bar{r}} (t_D - t_{DS})}{2 \sqrt{\frac{r_n}{\bar{r}} \alpha_D (t_D - t_{DS})}} \right) \text{ or} \quad (3)$$

$$C_D = \frac{a}{2} \operatorname{erfc} \left(\frac{x_D - \frac{H_K}{[1-(H_K-1)c]^2} t_D}{2 \sqrt{\frac{H_K}{[1-(H_K-1)c]^2} \alpha_D t_D}} \right) - \frac{a}{2} \operatorname{erfc} \left(\frac{x_D - \frac{H_K}{[1-(H_K-1)c]^2} (t_D - t_{DS})}{2 \sqrt{\frac{H_K}{[1-(H_K-1)c]^2} \alpha_D (t_D - t_{DS})}} \right)$$

where $c_D = \frac{c(x,t)-c_i}{c_j-c_i}$ is the dimensionless concentration; $c(x, t)$ is the concentration at any distance x and time t , c_i and c_j are the initial and injected concentrations (Bq/kgC), respectively; a is the dilution coefficient; $x_D = \frac{x}{L}$ is the dimensionless distance; x and L (m) are any distance and the inter-well spacing between the injector and producer; $t_D = \frac{ut}{L}$ is dimensionless time; u and t are interstitial velocity (m/d) and time (d); t_{DS} is the slug injection time; $\alpha_D = \frac{D_L}{uL} = \frac{1}{N_{pe}}$ is the dimensionless dispersivity normalized by the length of the permeable medium; D_L is the longitudinal dispersion coefficient, N_{pe} is the Peclet number, a dimensionless number which is the ratio of convection to diffusion transport mechanisms; $r_n = \frac{k_i}{\Phi_i}$ and $\bar{r} = \frac{\bar{k}}{\Phi}$ are the permeation velocity (m/d) of single-phase and average permeation velocities, respectively; k and Φ are the permeability ($10^{-3}\mu\text{m}^2$) and porosity (%), respectively; and H_K is the heterogeneity factor, indicating the complexity of the reservoir in the oil field.

The initial tracer injection data, the static data of the oil field, and the actual tracer response curve of the production well was inputted into a self-developed MATLAB program (Wei 2021). Then, according to the mathematical model of the tracer interpretation program, the theoretical response curve was calculated, and the fit parameters (a , α_D , r , and H_K) in the mathematical model were obtained, as shown in Table 1. Based on the established inter-well tracer monitoring interpretation model, the tracer production time and concentration of the production wells H136-2 and H136-8 were fitted, as shown in Figure 4.

Tracer Breakthrough Time and Water Drive Speed

Based on the tracer output concentration curve and the breakthrough time (T_b), and the inter-well spacing (L) between the injector and producer, the water drive speed was calculated according to the equation $v=L/T_b$, to be 6.6 m/d and 2.9 m/d for well H136-2 and H136-8, respectively, as shown in Table 2. The target-well group of the Hu 136 block is one of medium porosity and low permeability type well group. The original advancing speed of the main slug of the injected water is less than 2 m/d. Compared the data of drive speed monitored by the tracer with the original formation, it can be judged that dominant channels underground have been formed.

Distribution of Injected Water

The volume distribution coefficient of the injected water in the corresponding oil wells can be obtained according to the output concentration of the tracer in the corresponding oil well. It is assumed about 10% of the tracer is unrecovered. Therefore, when the injected water is distributed, the distribution ratio of each effective well is calculated as follows:

$$F = (A_i/\Sigma A_i) \times 0.9 \times 100\% \quad (4)$$

Table 1 Formation parameters obtained from the inter-well tracer interpretation model.

Well no.	Layer	Dilution coefficient: a ;	Dispersion coefficient: α_D	Heterogeneity factor: H_K	Average percolation velocity: \bar{r} (m/d)	Swept volume: V (m ³)	Average pore-throat radius: r (μ m)
H136-2	S3-1	0.8	0.12	1	1.2	575.35	3.10
	S3-2	0.6	0.015	1.19	2.6	920.34	4.56
	S3-3	0.55	0.01	1.3	2.3	326.29	4.29
H136-8	S3-1-3	0.38	0.0045	1	3.8	326.29	5.51
	S3-5	0.31	0.0042	1.05	3.9	605.43	3.9

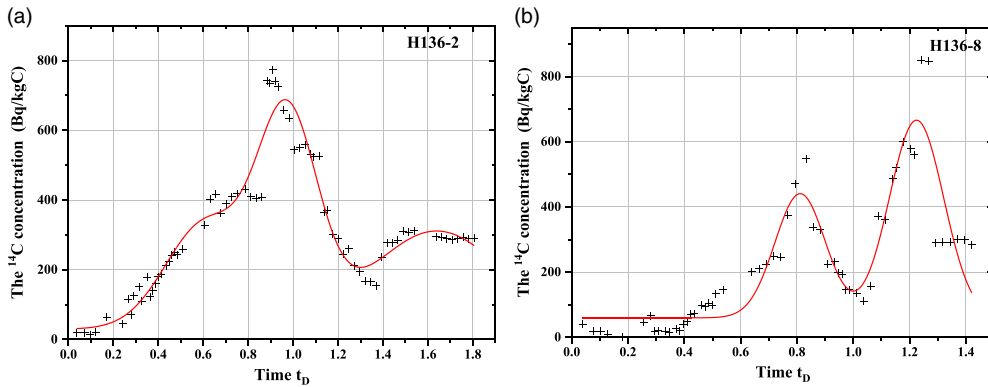


Figure 4 The dimensionless tracer concentration curve for well H136-2 (a) and H136-8 (b). The dot represents the dimensionless tracer concentration. The solid line represents the fit response curve.

where F is the proportion of injected water distribution (%), and A_i is the tracer output of each production well (g). The calculated results are listed in Table 3. It is clear that the main supply well was H136-2.

Swept Volume

According to the dilution factor a and peak concentration, each flow channel's water production and the swept volume between the injection and production wells can be calculated with the following formula group Eq. (5) (Shook and Foresmann 2005):

$$V = Q_C \times t_p, \quad Q_C = \left(\frac{c_i}{\sum_{i=1}^n c_i} \right) \times a \times Q_W \quad (5)$$

where V is the swept volume of the flow channel (m^3) and t_p is the peak time of the tracer. Q_C is the water production of the flow channel (m^3/d) and C_1 is the peak concentration of the tracer (Bq/kg) and Q_W is the daily water production of the production wells (m^3/d). The swept volume results are shown in Table 2. The relatively small swept volume of each flow channel, indicating that the utilization rate of the injection water is low, and there may be ineffective circulation of large pores or fractures between wells.

Heterogeneity

The heterogeneity factor H_K indicate the complexity of the reservoir in the oil field. The H_K value of the first geological sublayer of the production well H136-2 was 1, that of the second geological sublayer was 1.19, and that of the third geological sublayer was 1. The heterogeneity factor H_K of production well H136-8 in the first geological sublayer was 1 and that of the second geological sublayer was 1.05. The heterogeneity factor H_K of the two production wells is approximately 1, indicating that the reservoir is relatively homogeneous and there are high-permeability channels. This is consistent with the actual situation of slow advancement between the injection and production wells.

Table 2 Tracer response of H136-C1 well group.

Well no.	Well spacing (m)	Breakthrough time (d)	Drive speed (m/d)	Peak concentration times (d)	Peak concentration value (Bq/kgC)
H136-2	132	20	6.6	65, 77, 127	430, 740, 310
H136-8	156	54	2.9	92, 135	550, 850

Table 3 The Distribution of injected water in each well.

Well no.	Injection water distribution ratio (%)	Injection water distribution (m ³ /d)	Actual daily output (m ³ /d)
H136-2	62.6	28.17	39
H136-8	37.4	16.83	23.8

Average Pore Throat Radius

According to the cross-well tracer interpretation model, the average pore throat radius can be deduced based on Eq. (6) (He 1994).

$$r^* = \sqrt{\frac{8\bar{k}}{\bar{\phi}}} = \sqrt{8\bar{r}} \quad (6)$$

where r^* is the average pore throat radius, k is the average permeability, and ϕ is the average porosity. The average pore throat radius of the three permeable layers of well 136-2 is calculated to be 3.10 μm , 4.56 μm , and 2.3 μm , respectively, and that of the two permeable layers of well 136-8 is calculated to be 5.51 μm and 5.58 μm , respectively. According to the preliminary judgment standards for the development of large pores (Hu et al. 2006). It can be concluded that there are preliminarily developed large pores in the H136 well group.

CONCLUSIONS

The findings of this study provide a first look at the reservoir heterogeneity characteristics of ¹⁴C-AMS in China. We performed a 149-day radiocarbon tracer experiment for the Zhongyuan oil field located in central China. The corresponding relationship between the injection and production wells is clarified. The tracer can be seen in both the monitored wells (H136-2, H136-8), and the production concentration was relatively obvious. From the water absorption profile and perforation data, it is clear that the main supply well is H136-2. The advancing speed in the direction of the H136-2 well was 6.6 m/d, and 2.9 m/d in direction of H136-8. These results show the domination channel is H136-2. The five small layers between the injection and production wells were simulated, and it was calculated that there were high-permeability channels in the two small layers, including layers S3-2 and S 3-5, which were recommended to reconfigured and adjust the plugging. The ¹⁴C-AMS technique developed in this work is expected to be a potential analytical method for evaluating the remaining underground reservoir characteristics and providing crucial scientific guidance for the mid-late oilfield recovery process.

ACKNOWLEDGMENTS

This work was supported by the Guangxi Natural Science Foundation under Grant Nos. 2017GXNSFFA198016 and 2018JJA110037; the National Natural Science Foundation of China under Grant Nos. 11775057, 11765004, U1867212, 11965003, and 12164006; JSPS KAKENHI under Grant No. 21K18622; and Guilin Science and Technology Foundation Grant No. 20190209-2.

SUPPLEMENTARY MATERIAL

To view supplementary material for this article, please visit <https://doi.org/10.1017/RDC.2022.28>

REFERENCES

- Al-Fattah SM. 2020. Non-OPEC conventional oil: production decline, supply outlook and key implications. *Journal of Petroleum Science and Engineering* 189: 107049.
- Gao H, Tian X. 2009. Demonstration of water resources protection and utilization project in Puyang. *Science & Technology Information* 19:148–149.
- He G. 1994. *Reservoir physics*. Beijing: Petroleum Industry Press.
- He M et al. 2019. A home-made ^{14}C AMS system at CIAE. *Nuclear Instruments and Methods in Physics Research B* 438:214–217.
- Höök M, Hirsch R, Aleklett K. 2009. Giant oil field decline rates and their influence on world oil production. *Energy Policy* 37(6): 2262–2272
- Hu SY, Zhang LH, Luo JX, Luo GS, He J. 2006. Study on large pore path in sandstone reservoirs-review and prospect. *Special Oil and Gas Reservoirs* 13(6):10–14.
- Lake LW. 1989. *Enhanced oil recovery*. Englewood Cliffs, NJ: Prentice Hall.
- Rahimpur MR. 2004. A non-ideal rate-based model for industrial urea thermal hydrolyser. *Chemical Engineering and Processing: Process Intensification* 43(10):1299–1307.
- Sahu JN, Hussain S, Weikap BC. 2011. Studies on the hydrolysis of urea for production of ammonia and modeling for flow characterization in presence of stirring in a batch reactor using computational fluid dynamics. *Korean Journal of Chemical Engineering* 28(6):1380–1385.
- Shen H et al. 2019. Present status and application studies in GXNU-AMS Lab. The 8th East Asia Accelerator Mass Spectrometry Symposium, Nagoya, Japan.
- Shook GM, Forsmann JH. 2005. Tracer interpretation using temporal moments on a spreadsheet. Idaho National Laboratory.
- Wei SY. 2021. Study on Interwell tracer monitoring interpretation model in oil field [dissertation]. Guangxi Normal University.
- Zemel B. 1995. *Tracers in the oil field*. New York: Elsevier Science.
- Zhong T, Li G, Liu P, Shi F. 2008. Evaluation of tourism climate comfort in Puyang City. *Meteorological and Environmental Sciences* 31:129–130.